Quasi-elastic light scattering from branched polymers: 1. Polyvinylacetate and polyvinylacetate—microgels prepared by emulsion polymerization

Manfred Schmidt, Dittmar Nerger and Walther Burchard
Institute of Macromolecular Chemistry, University of Freiburg, West Germany
(Received 8 August 1978; revised 29 December 1978)

Emulsion polymerization of vinylacetate leads to branched polymers which at high monomer conversions form microgels of the shape and size of the latex particles. Quasielastic light scattering measurements from samples in the pre-gel state give at small q^2 a linear angular dependence of $D_{app} = \Gamma/q^2$ which resembles that of randomly branched chain molecules, where Γ is the decay constant of the time correlation function. Extrapolation of D_{app} towards zero scattering angle yields the translational diffusion constant D_z. The diffusion constant follows the molecular weight dependence $D_z = 9.78\ 10^{-5} M_w^{-0.478}$. The diffusion constant of the microgels, i.e. at molecular weights $M_w > 14\ 10^6$, remains constant because of the finite and constant size of the latex particles. The coefficients k_f and k_D in the concentration dependence of the frictional and diffusion coefficients are related according to the equation $k_D = k_f - 2A_2M_w - \bar{v}$ where A_2 is the second virial coefficient and $\bar{v}$ the partial specific volume of the particle. The coefficient k_f is calculated from the experimentally determined quantities k_D, A_2 and M_w, and the result is compared with the theory by Pyun and Fixman. Accordingly the branched coils in the pre-gel state resemble soft spheres, but the microgels behave more like spheres of some rigidity.

INTRODUCTION

Although photon correlation spectroscopy or quasielastic light scattering (QELS) is a fairly new technique in polymer science it has found a surprisingly deep resonance, and a vast number of papers on this subject has already been published[1–9]. Most of these studies deal with the determination of the translational diffusion constant D, and the application in biophysics and physical chemistry of polymers, results from the change of D when a macromolecule or biologic material undergoes a conformational transition and from the molecular weight and concentration dependence of D.

Quasielastic light scattering has, however, nothing to do with conventional diffusion measurements where an initial concentration gradient is the starting condition and the approach to equilibrium is followed. Instead, all types of motion of a Brownian particle from a system in thermodynamic equilibrium are observed. These types of motion include, besides the irregular translational motion, the irregular rotation of elongated particles and the internal modes of motion with respect to the centre of mass of a flexible particle. It is only because of the relatively small dimensions of the particles compared to the wave-length of the light used, that in most cases already investigated the translational diffusion constant only can be observed.

Early estimations by Pecora[10,11] have shown that for flexible chain molecules the internal motions will give a noticeable effect if the root mean square distance $\langle r_{ij}^2\rangle^{1/2}$ between two scattering elements i and j in a molecule is larger than $\lambda/2$, and a similar condition applies for the observation of a rotatory diffusion constant of elongated rigid particles[12]. Such large dimensions are rare in linear polymers and are found mainly with biopolymers[13–20] (DNA, RNA, Tobacco Mosaic Virus, Collagen). However, since the pioneering work by Flory and by Stockmayer[21–25] it is well known that very large macromolecules are obtained when branching occurs. These polymers – which can easily be prepared synthetically – fulfil the condition for the observation of internal modes of motion. The interpretation of the measurements is, on the other hand, rendered more difficult by the large polydispersity of most branched products and by the fact that the influence of branching on QELS was not known until this study has been started.

In recent papers the influence of polydispersity, of branching and of internal modes of motion has been studied experimentally and theoretically for some well defined models[26–30]. The results are summarized in the theoretical section and may serve as a guide for the interpretation of unknown branched systems e.g. like that obtained by emulsion polymerization of vinyl acetate.

The study of the vinylacetate emulsion polymerization has interest on its own. Because of the high chain transfer constant of the acetate groups from radical polymerization of vinyl acetate leads to highly branched samples and eventually to gelation. The point of gelation was predicted in

0032–3861/79/058205–07$02.00

bulk polymerization at 60° C to occur at about 80% monomer conversion[31]. Such a high conversion is difficult to achieve under control in bulk polymerization, but complete conversion is easily obtained in emulsion polymerization. In a series of runs at various temperatures of polymerization gelation could be indeed observed[32]. Some of these samples are used in the present study of QELS. These data give a first experimental basis for the determination of a gel point in a finite and microscopically small vessel.

THEORY

In quasielastic light scattering (QELS) a scattering intensity time-correlation function $G_2(t) = \langle i(\mathrm{O})i(t)\rangle$ is measured which in the so called homodyne technique is related to the electric field correlation function $g_1(t)^2$.

$$G_2(t) = \langle i(\mathrm{O})i(t)\rangle = A| + B|g_1(t)^2| \tag{1}$$

$$g_1(t) = \frac{\langle E(\mathrm{O})E^*(t)\rangle}{\langle |E(\mathrm{O})^2|\rangle} \tag{2}$$

In these equations $i(0)$ and $i(t)$ are the scattering intensities at times zero and t, respectively, and $E(\mathrm{O})$ and $E(t)$ the corresponding scattering electric fields where the asterisk denotes the conjugated complex quantity to $E(t)$. The constant A is a direct current and $B \leqslant 1$ is a constant which depends on the quantum efficiency of the photomultiplier used as a detector.

The correlation function $g_1(t)$ shows a simple exponential decay for rigid and monodisperse particles of spherical symmetry, but in all other cases $g_1(t)$ is a sum over a number of single exponential correlation functions. The initial part of the correlation function can still be well approximated by a single exponential which follows from the cumulant expansion of the sum[33,34]

$$g_1(t) = \sum_j g_i^{(j)}(t) \simeq e^{-\bar{\Gamma}t}(1 + \mu_2 t^2/2 \ldots) \tag{3}$$

with

$$\bar{\Gamma} = \Sigma\Gamma_j p(\Gamma_j) \tag{4}$$

$$\mu_2 = \Sigma(\Gamma_j - \bar{\Gamma})^2 p(\Gamma_j) \tag{5}$$

where $p(\Gamma_j)$ is the normalized distribution function of finding a special decay constant Γ_j.

The evaluation of the QELS data in the present study is confined to the determination of the initial decay constant Γ. Older theories deal mostly with the derivation of the correlation function $g_1(t)$ in terms of the various modes of motion[11–12,35–38]. Recently, however, Akcasu and Gurol[39] made use of a quite general relationship that can be derived (not solely with the linear projection operator technique) from Kirkwood's general differential equation of diffusion for a multicomponent system. This relationship is exact and based on no assumption, so far as Kirkwood diffusion equation can be considered to be exact. In particular no specific assumption on the interaction potential is needed in contrast to Pecora's treatment of flexible chains where the typical square potential of the spring bead model had to be assumed explicitly.

Application of the Akcasu–Gurol treatment in combination with Gordon's cascade theory to polydisperse linear and branched chains[40,41] allowed the derivation of the initial decay constant as a function of the scattering angle for various models where hydrodynamic interaction between segments were taken into account[27,28]. Although these models cannot be applied strictly to PVAc the results of the calculations show some surprising common features which at least can be taken as a guide for the interpretation of more complex systems. Since these common properties have been summarized already elsewhere[29] and since only the region of small values of the scattering vector q are accessible with PVAc, mention will be made of the behaviour at low q-values.

(a) For all types of flexible chains considered so far (linear or branched) we found for small q[29]

$$\frac{\bar{\Gamma}}{q^2} \equiv D_{app} = D_z(1 + c_1\langle S^2\rangle_z q^2 \ldots) \tag{6}$$

where

$$q = (4\pi/\lambda)\sin\theta/2 \tag{7}$$

with λ the wave-length in the medium and θ the scattering angle. In other words, a plot of the apparent diffusion coefficient against q^2 should give a straight line with intercept D_z, which is the z-average diffusion coefficient, and slope $\langle S^2\rangle_z$, the z-average mean-square radius of gyration. The constant c_1 is model dependent and is $c_1 = 1/6$ for randomly branched polycondensates and can change down to $c_1 = 1/12$ if the branching process is confined to certain restrictions.

(b) The z-average diffusion coefficient is proportional to the reciprocal radius of gyration

$$D_z = \frac{kT}{\eta_0} \times \frac{c_3}{c_1^{1/2}} \Big/ \langle S^2\rangle_Z^{1/2} \tag{8}$$

where c_3 depends significantly on the mean segment density and the shape of the segment density distribution around the centre of mass; to some extent it also depends on the polydispersity. The coefficient $(c_3/c^{1/2})$ is therefore a factor sensitive to the internal structure.

(c) In a randomly branching system one has under θ-conditions

$$D_z \sim M_w^{-1/2} \tag{9}$$

EXPERIMENTAL

The polymers used in this study were prepared by emulsion polymerization of vinyl acetate at 20°C and 10°C under conditions described in a separate paper[42]. The latex samples were withdrawn from the reactor at different monomer conversions and immediately coagulated by freezing. The precipitate was wrung and washed on a suction filter with ice-water until no foam formation could be observed. The precipitate was dissolved in methanol and reprecipitated into ice-water. This procedure was repeated twice or three times in order to remove adsorbed residues of the emulsifiers. The polymer was dried in vacuum with silica gel at temperatures below 20°C. For further details of the preparation and working up of the polymers see

Table 1 Molecular weight M_w, translational diffusion constant D_z, mean square radius of gyration $\langle S^2\rangle_z$, and 2nd virial coefficient of PVAC polymerized in emulsion and measured in methanol at 25°

Sample	$M_w \times 10^{-6}$	$D_z \times 10^8$ cm^2 sec^{-1}	$\langle S^2\rangle_z \times 10^{10}$ cm^2	$A_2 \times 10^5$ cm^3 mol/g^2	$D_z\langle S^2\rangle_z^{1/2} \times 10^{14}$	$\langle R_s^{-1}\rangle_z\langle S^2\rangle_z^{1/2}$
109	2.36	8.6	0.739	7.50	7.39	1.853
82	4.18	6.5	1.25	5.24	7.27	1.821
88	7.16	4.8	2.21	4.96	7.13	1.788
146	10.60	4.3	2.49	1.85	6.79	1.699
113	17.5	3.4	2.84	2.31	5.73	1.436
136	31.7	1.6	2.21	1.35	2.38	0.596
139	74.4	1.6	2.04	0.367	2.29	0.573
116	262.2	1.6	1.95	0.107	2.23	0.560
149	422.9	1.6	1.87	0.172	2.18	0.548

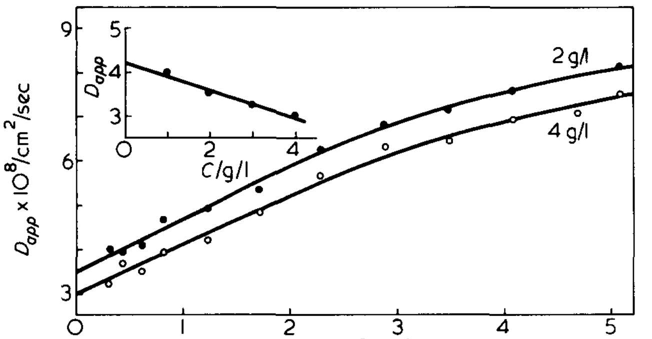

Figure 1 Typical angular dependence of the apparent diffusion constant $D_{app} = \Gamma/q^2$ for a PVAC sample ($M_w = 10.6 \times 10^6$) which has not yet gelled in the latex particle

reference 42. The monomer conversion was determined gravimetrically by freeze drying an aliquot of the original latex suspension.

Molecular weights and mean square radii of gyration were determined by elastic light scattering using the Fica 42 000 photo goniometer. Details of these measurements and the dependence on the monomer conversion are given in reference 42.

All quasielastic light scattering measurements were performed with the Malvern Autocorrelator K7023 equipped with 48 channels and with the RR 102 photo goniometer. The light source was a 15 mW He Ne laser of Spectra Physics. A low dark current and low correlation time photomultiplier ITT FW 130 was used as a detector, (dark current about 20 counts per second). The time correlation measurements were performed at 25°C and at 10–12 different angles in the range from 15 to 120 angle degrees. U.v. spectroscopy grade methanol was used as solvent, and the concentration dependence was followed at 4–9 concentrations in the range of 0.2–4.0 g/l.

Special care was given to the clarification of the solutions to make the solutions dustfree. Because of the high molecular weights only the first three samples in Table 1 were centrifuged in a Spinco ultracentrifuge model L; all other samples were clarified by filtration through millipore filters of 680 nm pore size.

RESULTS

Figures 1 and *2* give examples for the angular dependence of the apparent diffusion constant which is the initial decay constant $\bar{\Gamma}$ of the time correlation function divided by $q^2 = (4\pi/\lambda)^2 \sin^2 \theta/2$. These two examples show converse behaviour; in *Figure 1* a rectilinear initial part is obtained with a downturn at higher q^2 values, while in *Figure 2* an upturn at low q^2 is found and a nearly rectilinear behaviour at larger q^2. For reasons described below these two examples are assigned to states before and after gelation had taken place within the latex particle. All samples in the pregel state show behaviour of *Figure 1* and all samples in the postgel state show that of *Figure 2*.

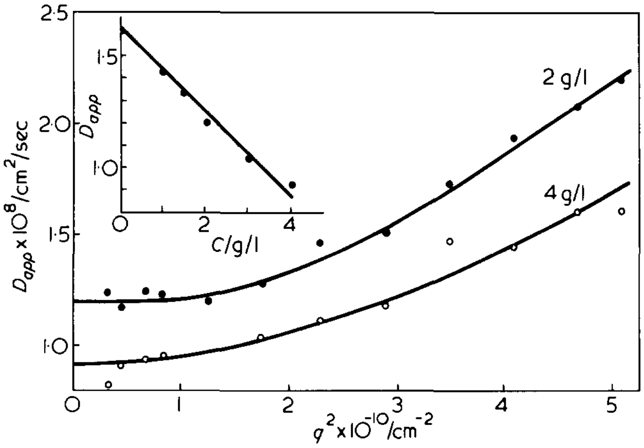

Figure 2 Typical angular dependence of the apparent diffusion constant for a sample ($M_w = 31.7 \times 10^6$) that has gelled in the latex particle

The intercept of the D_{app} extrapolated towards $q^2 \to 0$ curve gives the z-average translational diffusion constant. (Since the branched samples have essentially spherical outer shape and no detectable anisotropy there is no effect from a rotational diffusion constant). The diffusion constant D_z depends on the molecular weight which is shown in *Figure 3*. The full circles represent the points of QELS measurements while the open circles are results obtained by Elias[43] by conventional diffusion experiments in butanone. The original measurements follow the dotted line in *Figure 3*, but when the data are corrected for the difference in the viscosity of methanol and butanone

$$D_z^{\text{methanol}} = \frac{\eta_0^{\text{butanone}}}{\eta_0^{\text{methanol}}} D_z^{\text{butanone}} \tag{10}$$

the values of the open circles are obtained. (Note that always $D \sim 1/\eta_0$). Up to a molecular weight of $M_w = 14 \times 10^6$ the diffusion constant follows the relationship

$$D_z = 9.78 \times 10^{-5} M_w^{-0.478}, \text{cm}^2/\text{sec} \tag{11}$$

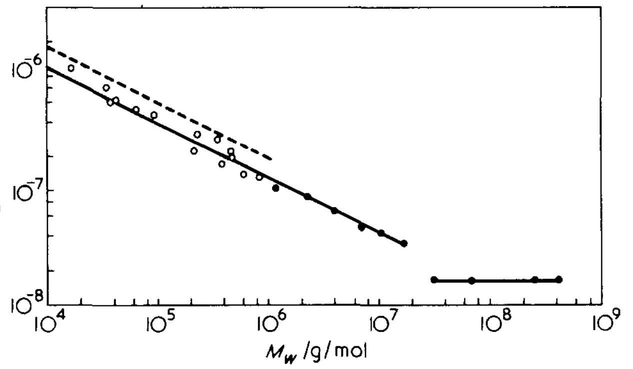

Figure 3 Molecular weight dependence of the translational diffusion constant of PVAC in methanol at 25° centigrade; ● measured by QELS; ○ data of Elias obtained by conventional techniques after correction for the difference in viscosity of butanone and methanol; dotted line: original measurements of PVAC from bulk polymerization by Elias

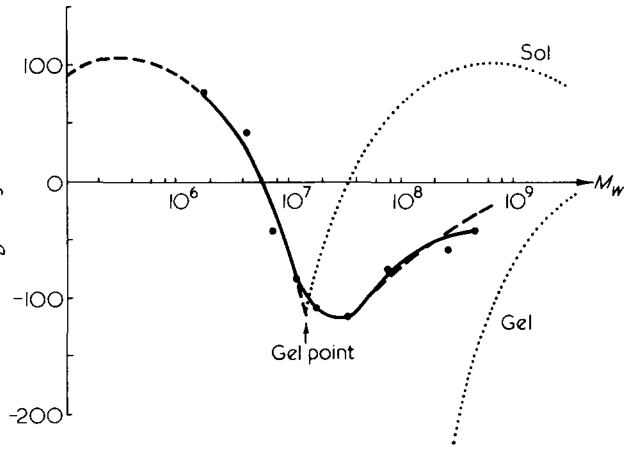

Figure 4 Molecular weight dependence of the coefficient k_D in the concentration dependence of $D_z + k_D = 2A_2M_w - k_f$

but for larger molecular weights ($M_w \geqslant 14 \times 10^6$) it remains constant

$$D_z = 1.6 \times 10^{-8}, \text{cm}^2/\text{sec} \qquad (12)$$

In all cases a concentration dependence of the diffusion constant was observed which follows for sufficiently small concentrations the familiar relationship

$$D_z(c) = D_z(1 + k_D c) \qquad (13)$$

The coefficient k_D varies considerably with the molecular weight from positive values at low molecular weights to negative values for the high molecular weights. The inserts in *Figures 1* and *2* show the concentration dependence for two examples. The dependence of k_D on M_w is given in *Figure 4*.

DISCUSSION

Before the results are discussed in detail it may be useful to summarize some important facts.

(1) The molecular weight dependence of the translational diffusion constant shows a kink around a molecular weight of $M_w = 15 - 25 \times 10^6$. Below this region D_z decreases with M_w, but for larger molecular weights D_z remains constant.

(2) The coefficient k_D which describes the concentration dependence of the diffusion constant at low concentration exhibits a minimum in the range of $M_w = 15 - 60 \times 10^6$.

(3) The quasielastic scattering changes behaviour when a molecular weight of $M_w = 15 - 20 \times 10^6$ is exceeded.

Adding to these points the findings that also the mean square radius of gyration $\langle S^2\rangle_z$, the intrinsic viscosity and the elastic scattering change behaviour around the molecular weight of 15×10^6 one is lead to the conclusion that this molecular weight has the characteristics of a critical point. Since gelation is expected for PVAC this critical point can be taken as the gel point where gelation takes place within the latex particle. Conclusive proof of this interpretation is given in references 32 and 42; in the present discussion we will check as to whether the QELS results are in accordance with this concept.

The translational diffusion constant

In a freely branching system the molecular weight and the size of the molecules grow continuously as the branching process proceeds. For random branching processes this growth follows the equation[23,31,44]

$$\frac{P_w}{P_{wo}} = \frac{1+\gamma}{1-\gamma/\gamma c} \qquad (14)$$

where γ is the branching probability which depends on the monomer conversion and P_{wo} is the degree of polymerization of a linear primary chain which is created in each chain reaction of the free radical polymerization.

The branching process of PVAc is somewhat more complex but equation (10) can still be considered as a good approximation also for this sytem[31]. At a critical branching density γc the degree of polymerization P_w increases beyond limits, and a macroscopic gel is formed. Since the mean square radius of gyration $\langle S^2\rangle_z$ is proportional to P_w one has, for a macroscopic system at the gel point, $P_{wc} \to \infty$, $\langle S^2\rangle_{zc} \to \infty$ and $D_{zc} = 0$. Such behaviour is not observed for the finite system of PVAc, and D_z decreases in the expected manner only until a molecular weight of $M_w = 15.10^6$ is reached and then remains constant. Obviously some of the branched molecules have reached a size which extends all over the space of the latex particle. On further reaction the radii of the gelled macromolecules cannot grow further, but unreacted monomers and the smaller molecules from the sol can be attached to this gel fraction and will cause an increase of the overall weight average particle weight. Since $\langle S^2\rangle_z$ does not change during that process necessarily D_z of the microgel must remain constant.

The diffusion coefficient of a hard sphere is proportional to the inverse sphere radius. Similarly one can define a formal Stokes radius.

$$D_z = \frac{kT}{6\pi\eta_0}\left\langle\frac{1}{R_s}\right\rangle_z \qquad (15)$$

The product $D_z\langle S^2\rangle_z^{1/2}$ or $\langle R_s^{-1}\rangle_z\langle S^2\rangle_z^{1/2}$ is evidently a quantity that no longer depends on the molecule dimensions, but is of course, still dependent on the polydispersity[29]. It also depends on the structure and shape of the particles because the mean square radius of gyration is a geometrical average over the size of the particle while R_s is a hydrodynamically effective radius. For linear and randomly branched flexible chains under theta conditions one has[27,54]:

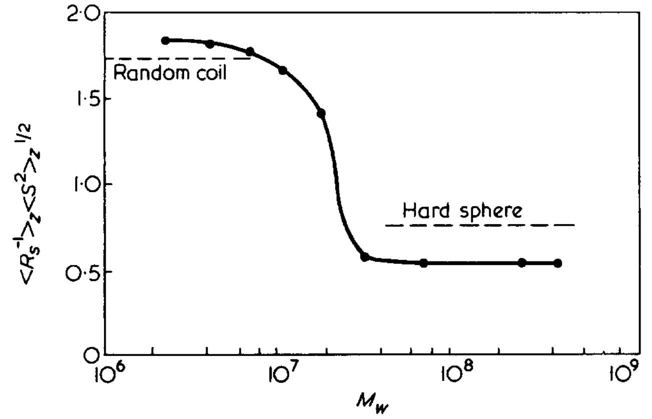

Figure 5 The variation of $\langle R_s^{-1}\rangle_z\langle S^2\rangle_z^{1/2}$ with M_w. The dotted lines indicate the values for flexible and random coils and for hard spheres respectively

$$\langle R_s^{-1}\rangle_z\langle S^2\rangle_z^{1/2} = 1.730 \qquad (16)$$

and for monodisperse hard spheres of constant density (since $\langle S^2\rangle = 3/5\,R^2$)

$$\langle R_s^{-1}\rangle_z\langle S^2\rangle_z^{1/2} = 0.775 \qquad (17)$$

The plot of this quantity in *Figure 5* for the nine points of measurements against the molecular weight reveals a marked change around $M_w = 15 \times 10^6$ which most instructively indicates the transition from a randomly branched molecule to a solidified sphere. The somewhat higher value of 1.85 at low molecular weights may result from the effect of excluded volume or from experimental errors which might be large since D_z and $\langle S^2\rangle_z$ have been measured with different instruments. The values at high molecular weights which are by 23–30% lower than that for compact spheres appears to be out of the range of experimental errors and is probably an indication for a special spatial density distribution in the microgel. The apparently larger Stokes radius in comparison to the mean square radius of gyration of a hard sphere may for instance result from a crosslinked thin surface layer which has a much lower density than the microgel centre but which may suffice to define a hydrodynamically effective large sphere radius while the mean square radius of gyration remains fairly small. This is illustrated by the sketch of *Figure 6*.

The concentration dependence of D_z

The concentration dependence of the translational diffusion constant is influenced by both thermodynamic and hydrodynamic interactions and can be described by linear relationships

$$\frac{1}{M_{app}} = \frac{1}{M_w}(1 + 2A_2M_wc) \qquad (18)$$

$$f = f_0(1 + k_fc) \qquad (19)$$

$$D = D_0(1 + k_Dc) \qquad (13)$$

where M_{app} is the apparent molecular weight at a given concentration and A_2 is the second virial coefficient.

Irreversible thermodynamics prove that the three coefficients $2A_2M_w$, k_f and k_D are related[45]

$$k_D + k_f = 2A_2M_w - \bar{v} \qquad (20)$$

The partial specific volume $\bar{v}$ of the polymer in solution is in the order of one and by orders of magnitude smaller than $2A_2M_w$, it may be neglected in most cases. In equation (28) k_D can be measured by means of QELS and A_2 by conventional light scattering. *Figure 7* shows the molecular weight dependence of A_2 which follows the relationship

$$2A_2M_w = 10.8\,M_w^{0.238},\ \mathrm{cm^3/g} \qquad (21)$$

The second virial coefficient shows no detectable kink around the critical molecular weight of $M_w = 15 \times 10^6$. This behaviour probably arises from the low accuracy to which A_2 can be measured.

The coefficient k_f has been calculated theoretically by several authors[46–48] and agree in so far that[49;50]

$$k_f = k_{f0}\frac{N_A\,V_h}{M_w} \qquad (22)$$

where k_{f0} is the frictional coefficient at theta conditions and V_h is the hydrodynamic volume which may be calculated from the diffusion constant setting the hydrodynamic radius equal to the Stokes radius R_s (the Stokes radius is defined in equation (23)).

$$V_h = \frac{4\pi}{3}\left(\frac{kT}{6\pi\eta_0D_z}\right)^3 \qquad (23)$$

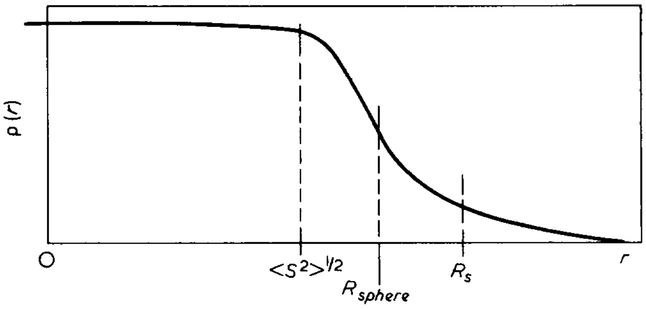

Figure 6 Possible density distribution $\rho(r)$ of a microgel and the position of the radius of gyration $\langle S^2\rangle^{1/2}$, Stokes radius R_s and the average sphere radius R_{sphere}. Due to this mode. one has $\langle R_s^{-1}\rangle\langle S^2\rangle^{1/2} = 0.6$

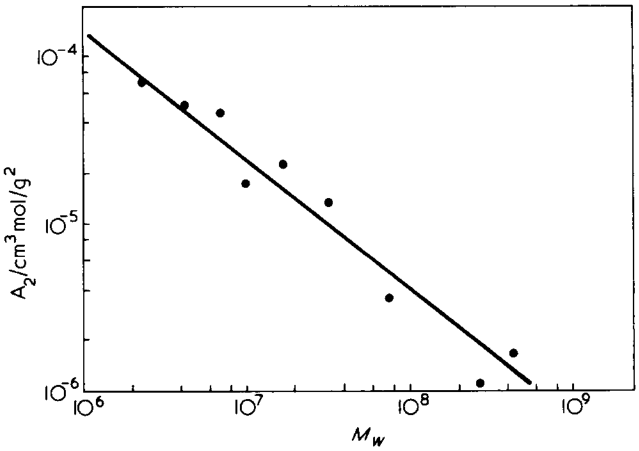

Figure 7 Molecular weight dependence of the second virial coefficient for PVAC polymerized in emulsion and measured in methanol ($A_2 = 5.4\,M_w^{-0.762}$)

Table 2 Molecular weight M_w, coefficient k_D in the concentration dependence of the translational diffusion constant and 2nd virial coefficient of PVAC polymerized in emulsion and measured in methanol

Sample	$M_w \times 10^{-6}$	k_D cm^3/g	$A_2 \times 10^5$ cm^3 mol/g^2
109	2.36	96	7.50
82	4.18	40	5.24
88	7.16	−44	4.96
146	10.66	−83	1.85
113	17.5	−107	2.31
136	31.7	−115	1.35
139	74.4	−73	0.367
116	262.2	−57	0.107
149	422.9	−50	0.177

With the use of equation (17) for the molecular weight dependence of D_z equation (30) becomes

$$k_f = k_{fo} \times 0.207 M_w^{0.434} \tag{24}$$

There is no full agreement between the various theories on the value of k_{fo}; we refer here to the theory of Pyun and Fixman[47]. These authors find

$$k_{fo} = 7.16 \text{ for the hard sphere}$$

$$k_{fo} = 2.23 \text{ for the soft sphere} \tag{25}$$

The term soft sphere needs some explanation. Pyun and Fixman used for their calculations the Flory–Krigbaum model[51] of interpenetrable spheres of segments clouds. With increasing second virial coefficient the repulsion between the segments offers resistance against penetration and makes the spheres more rigid until in the limit of strong interactions the hard sphere results. Solidification of a coil may on the other hand also be caused by branching or slight crosslinking, and therefore we consider the k_{fo}-values as a measure of the internal rigidity of a spherical particle.

Using the $k_{fo} = 2.23$ value of the soft sphere at theta temperature one obtains

$$k_o = 0.462 M_w^{0.434} - 10.8 M_w^{0.238} \tag{26}$$

and the chain curve in *Figure 4*, which fits the experimental curve nicely up to a molecular weight of about $M_w = 11 \times 10^6$. For freely branched molecules k_o would decrease further with increasing M_w. At $M_w = 14 \times 10^6$, however, the microgel formation commences, and the molecular weight dependence of k_D for these microgels can be expected to be different.

The following estimation is very approximate and is a tentative interpretation. First one has to recall that a microgel contains a certain sol fraction which consists of molecules which are smaller in size than the corresponding latex particles. The sol fraction decreases from 1 to zero as the crosslinking reaction proceeds[25]. Simultaneously the molecular weight and the mean square radius of gyration of the molecules from the sol decrease[31, 52, 53]. The sol fraction was quantitatively determined by gel permeation chromatography. The calculation of k_D can now be performed under the following assumptions.

(i) *Gel fraction*: The particles of the gel fraction are spheres which are not completely rigid. The k_{fo}-value in equation (33) is expected to lie between 2.23 and 7.16. The second virial coefficient is that of spheres and follows the equation[45]:

$$2A_2M_w = \frac{16\pi}{3} N_A \left(\frac{3}{5} R_s^2\right)^{3/2} / M_w$$

$$= 14.53 \times 10^{10}/M_w \tag{27}$$

where the Stokes radius $R_s = 2.49 \times 10^{-5}$ cm of the microgel spheres has been used. Collecting equations (20), (22), (23) and (27) one has

$$k_D^{\text{gel}} = (k_{fo} \times 3.89 - 14.53) 10^{10}/M_w \tag{28}$$

(ii) *Sol fraction*: In a plot of P_w against γ/γ_c one finds for a random and free branching process a nearly symmetric curve around γ_c, i.e. the degree of polymerization decreases sharply in the same way for $\gamma_c - \Delta\gamma$ and for $\gamma_c + \Delta\gamma$[53]. We thus assume in this coarse estimation that k_D^{sol} follows the dotted line in *Figure 4* which is the mirror curve to the k_D dependence in the pregel state.

(iii) *Superposition of sol- and gel-fractions*: The experimentally observable k_D curve is composed of the two fractions as

$$k_D^{total} = k_0^{gel} m_{gel} + k_D^{sol}(1 - m_{gel}) \tag{29}$$

where k_D^{gel} is given by equation (28) and k_D^{sol} by the dotted line in *Figure 4*. Since the gel fractions of the microgels, m_{gel} are known from g.p.c. (*Table 2*) the k_{fo} value can be calculated with equation (28) from the experimental k_D-values. The best fit (chain curve in *Figure 4*) is obtained with $k_{fo}^{gel} \simeq 5$ (dotted line) which is a physically reasonable value and would indicate the microgel particles as a moderately soft sphere.

This estimation is, as already emphasized, very approximate and needs a critical examination. Without any doubt it can be stated, (i) the sol fraction decreases sharply with M_w of the system, and k_D is finally determined solely by the properties of the gel fraction; (ii) the k_D^{gel} values decrease with M_w whatsoever the k_{fo} value in equation (28) is. Thus a behaviour as indicated by the chain curve in *Figure 4* is inevitable. Furthermore, it turns out that the exact molecular weight dependence of k_D^{sol} has only little influence on k_D^{total}, but the latter is sensitively dependent on the value of k_{fo}^{gel}. We therefore believe that a more refined calculation will change this value only inessentially.

The angular dependence of D_{app}

As already pointed out in the theoretical section the apparent diffusion constant of a randomly branched polymer should yield a linear initial part when D_{app} is plotted against q^2. This behaviour is indeed observed for all samples below $M_w = 14 \times 10^6$ but not for the samples above this critical molecular weight. These findings are in the line with the picture of molecules which are not hindered in their growth as long as these molecules are smaller in size than the latex particles.

The behaviour of the microgels is unexpected, and at present we cannot offer an exhaustive explanation. What we know is that hard but polydisperse spheres will show a certain angular dependence of D_{app}[28–30], and a linear dependence on q^2 is in fact found for the latex particles which have a certain size distribution. The size distribution of the corresponding microgels is much broader, and therefore a stronger angular dependence will result which needs not to be linear at larger q^2-values. Still we think it unlikely that the marked upturn in *Figure 2* is caused by the polydispersity alone. The upturn may arise in our opinion from a certain flexibility of the microgels, because in random coils the angular dependence at large q-values is determined predominantly by its flexibility[29,38,39]. The conclusion of a more or less soft sphere would be in agreement with the analysis of the concentration dependence of D_z. Unfortunately no theory for soft spheres is available which would allow a more quantitative interpretation of angular dependence of the quasielastic light scattering measurements from the microgels.

ACKNOWLEDGEMENTS

We are indebted to the Deutsche Forschungsgemeinschaft who supported this research work.

REFERENCES

1 Chu, B. 'Laser Light Scattering', Academic Press, New York, 1974
2 Berne, B. J. and Pecora, R. 'Dynamic Light Scattering', J. Wiley, New York, 1976
3 Cummins, H. Z. and Pike, E. R. 'Photon Correlation Spectroscopy and Light Beating Spectroscopy', Plenum Press, New York – London 1974
4 Cummins, H. Z. and Pike, E. R. 'Photon Correlation Spectroscopy and Evlocimetry', Plenum Press, New York–London 1977
5 Berne, B. J. and Pecora, R. *Ann. Rev. Phys. Chem.* 1974, **25**, 233
6 Chu, B. *Ann. Rev. Phys. Chem* 1970, **21**, 145
7 Pecora, R. *Ann. Rev. Biophys. Bioeng.* 1972, **1**, 257
8 Ford, N. C., Gable, R. and Karasz, F. E. *Adv. Chem.* 1973, **125**, 26
9 Ford, N. C. *Chemica Scripta* 1972, **2**, 193
10 Pecora, R. *J. Chem. Phys.* 1964, **40**, 1604
11 Pecora, R. *J. Chem. Phys.* 1965, **43**, 1562
12 Pecora, R. *J. Chem. Phys.* 1968, **48**, 4126
13 Jolly, D. and Eisenberg, H. *Biopolymers* 1976, **15**, 61
14 Schmidt, R. L. *Biopolymers* 1973, **12**, 1427
15 Schmitz, K. S. and Schurr, J. M. *Biopolymers* 1973, **12**, 1543
16 Schmitz, K. S. and Pecora, R. *Biopolymers* 1975, **14**, 521
17 Wada, A., Ford, N. C. and Karasz, F. E. *J. Chem. Phys.* 1971, **55**, 1798
18 Schaefer, D. W., Benedek, G. B., Schofield, P. and Bradford, E. *J. Chem. Phys.* 1971, **55**, 3884
19 Schurr, J. M. and Schmitz, K. S. *Biopolymers* 1973, **12**, 1021
20 Lee, W. I., Schmitz, K. S., Lin, S. -Ch. and Schurr, J. M. *Biopolymers* 1977, **16**, 583
21 Flory, P. J. *J. Am. Chem. Soc.* 1941, **63**, 3083
22 Stockmayer, W. H. *J. Chem. Phys.* 1943, **11**, 45
23 Stockmayer, W. H. *J. Chem. Phys.* 1944, **12**, 125
24 Flory, P. J. *Chem. Rev.* 1946, **39**, 133
25 Flory, P. J. 'Principles of Polymer Chemistry', Cornell University Press, Ithaca, 1953, Ch 3 and 9
26 Schmidt, M., Burchard, W. and Ford, N. C. *Macromolecules* 1978, **11**, 452
27 Burchard, W. *Macromolecules* 1978, **11**, 455
28 Schmidt, M. and Burchard, W. *Macromolecules* 1978, **11**, 460
29 Burchard, W. *Polymer* (submitted)
30 Burchard, W. *Polymer* (submitted)
31 Wolf, Ch. and Burchard, W. *Makromol. Chem.* 1976, **177**, 2519
32 Nerger, D. and Burchard, W. manuscript in preparation
33 Koppel, D. E. *J. Chem. Phys.* 1972, **57**, 4814
34 Pusey, P. N., Koppel, D. E., Schaefer, D. W., Camerini-Otero, R. D. and Koenig, S. H. *Biochemistry* 1974, **13**, 952
35 Rouse, P. E. *J. Chem. Phys.* 1953, **21**, 1272
36 Bueldt, G. *Macromolecules* 1976, **9**, 606
37 Zimm, B. H. *J. Chem. Phys.* 1956, **24**, 269
38 Dubois-Violette, E. and de Gennes, P. -G. *Physics* 1967, **3**, 181
39 Akcasu, Z. and Gurol, H. *J. Polym. Sci. Phys.* 1976, **14**, 1
40 Kajiwara, K., Burchard, W. and Gordon, M. *Br. Polym. J.* 1970, **2**, 110
41 Burchard, W. *Macromolecules* 1977, **10**, 919
42 Nerger, D. *Ph. D. Thesis* Freiburg 1978
43 Elias, H. G. and Patat, F. *Makromol. Chem.* 1958, **25**, 13
44 Dobson, G. R. and Gordon, M. *J. Chem Phys.* 1965, **43**, 705
45 See for instance: Yamakawa, H. 'Modern Theory of Polymer Solutions', Harper and Row, New York 1971, Ch 6
46 Yamakawa, H. *J. Chem. Phys.* 1962, **36**, 2995
47 Pyun, C. W. and Fixman, M. *J. Chem. Phys.* 1964, **41**, 937
48 Imai, S. *J. Chem. Phys.* 1969, **50**, 2116
49 See also: King, T. A., Knox, A., Lee, W. I. and McAdam, J. D. *Polymer* 1973, **14**, 151
50 Vrentas, J. S. and Duda, J. L. *J. Polym. Sci.* 1976, **14**, 101
51 Flory, P. J. and Krigbaum, W. R. *J. Chem. Phys.* 1950, **18**, 1086
52 Burchard, W., Ullisch, B. and Wolf, Ch. *Faraday Discuss. Chem. Soc.* 1974, **57**, 56
53 Eschwey, H. and Burchard, W. *J. Polym. Sci. (C)* 1975, **53**, 1
54 The Stokes radius is $\langle R_s^{-1}\rangle_z = 6\pi D_z(\eta_0/kT)$. Hence from equation (12) one finds for random coils $\langle R_s\rangle_z\langle S_z^2\rangle^{1/2} = 1.730$. For hard monodisperse spheres the sphere radius equals the hydrodynamic radius, and the relationship between the mean square radius of gyration and the Stokes radius is $R_s = R_{sphere} = [(3/5)\langle S^2\rangle]^{1/2}$ or $\langle R_s^{-1}\rangle\langle S^2\rangle^{1/2} = 0.775$